2015 IEEE Intelligent Vehicles Symposium (IV)
June 28 - July 1, 2015. COEX, Seoul, Korea

How to predict real road state from vehicle embedded camera?

N. Gimonet [1], A. Cord[2], G. Saint Pierre[2]

Abstract— **Advanced Driver Assistance Systems (ADAS) based on video camera are increasingly invasive in todays car. However, if most of these systems work properly under clear weather, their performances drastically fall in case of adverse weather or bad lighting conditions. In this paper we study how to predict the road state: wet or dry. We simulate realistic embedded images relying on scene's physical data: road's Bidirectional Reflectance Distribution Function (BRDF) , vehicle direction, sun position and daylight model of the sky. These data are used to produce a database of 640 synthetic images of wet and dry road scene, under different conditions (weather, date, direction). This database allows us to evaluate the relationship between conditions and road state, in order to determine from a given condition if the road state could be predictable. Finally, an optimization method is used to estimate road surfaces' BRDF parameters.**

I. Introduction

Advanced Driver Assistance Systems (ADAS) based on video camera are increasingly invasive in today's cars : Lane Departure, Forward Collision Warning, Adaptative Headlight Control or Road Sign Detectors. Most of those systems are developed to work under clear visibility conditions. However, under adverse weather conditions, such as rain, snow, or fog, their performance are heavily affected. Moreover, such weather conditions strongly impact the driver safety by reducing both the visibility distance and the tire grip. Therefore, when the driver really needs assistance, some ADAS failures may occur.

For a system, the development of specific algorithms for each different weather condition is very fastidious. Therefore, reliable detection and characterization of adverse conditions is needed to compensate for the lack of camera based systems. By using the same vision sensor, systems should be able to evaluate their reliability and extend their functionality. Moreover, it could lead to new ADAS by, for instance, alerting the driver if his behavior is inappropriate for current driving conditions.

In this paper, we want to study the possibility to automatically predict the road state : wet or dry. This information is critical to ensure driver safety and to provide him information, in particular in case of excessive speed. For this purpose, we simulate realistic images from an embedded camera, varying different parameters: sky luminance properties (depending on the weather), date, time and vehicle direction (cap). By evaluating the differences between wet and dry roads images, we investigate which parameters are critical for the prediction of the road state.

This paper is organized as follows. In Section II, we describe physically-realistic image simulation. The results are detailed in Section III. Discussion and conclusion are in Section IV.

II. How to simulate an image

An image simulation relies on geometrical knowledge of the scene : camera position and flat world assumption. It also needs:

1) the solar position (relative to the vehicle);
2) the sky illuminance;
3) the road bidirectional reflectance distribution function (BRDF).

All those elements are presented in the current Section.

A. Solar position

Basing on an accumulation over time of Global Positioning System data (GPS), it is possible to estimate the vehicle position and direction. Combined with the time and the date, it is used to calculate the solar position relatively to the car, through a method proposed by [1]. The solar position is defined by two angles :

- the solar altitude, corresponding to the angular height above the horizon (or its complementary angle called the zenith angle).
- the azimuth, which is the angle between its projection in the horizontal plane and the geographic north (clockwise measured).

This model precision is smaller than 1° in azimuth and zenith and has a small computational cost. For all those reasons, it was preferred to two other classical models from Grena [2] or Van Flandern [3].

B. Sky model

The sky model corresponds to the light emitted by the whole sky. It exists two main models to evaluate it. First, the International Commission on Illumination [4] proposed a classification of 16 types of weather: from blue sky to very cloudy sky via polluted sky. However, the identification of the weather type, and the transition between two types may cause difficulties. Secondly, the "all-weather" model proposed by Perez ([5], [6], [7], [8]) relies on measurable illuminance parameters. We adopted this model, which is detailed in the following.

The Perez model introduces the relative luminance, lv, defined as the ratio between the luminance of the considered

[1] Nicolas Gimonet is PhD student in the institute IFSTTAR - LIVIC. IFSTTAR - LIVIC, 77 rue des chantiers, 78 000 Versailles, France nicolas.gimonet@ifsttar.fr

[2] Aurlien Cord and Guillaume Saint Pierre are researchers in the institute IFSTTAR - LIVIC. IFSTTAR - LIVIC, 77 rue des chantiers, 78 000 Versailles, France (aurelien.cord, guillaume.saintpierre)@ifsttar.fr@ifsttar.fr

sky element and the luminance of an arbitrary reference sky element (generally zenith luminance):

$$lv = \left[1 + a\exp\left(\frac{b}{\cos\xi}\right)\right]\left[1 + c\exp(d\gamma) + e\cos^2\gamma\right] \quad (1)$$

where ξ = zenith angle of the considered sky element;
γ = angle between the sky element and the sun;

The parameters a, b, c, d and e are calculated from two measurements : ε (sky clearness) and Δ (sky brightness). The calculation of these five parameters is detailed in [7], [8].

According to [4],γ is defined by:

$$\gamma = \arccos(\cos\xi_s \cdot \cos\xi + \sin\xi_s \cdot \sin\xi \cdot \cos|\alpha - \alpha_s|) \quad (2)$$

where ξ_s = zenith angle of the sun
α_s = azimuth of the sun
α = azimuth of the considered sky element

C. Bidirectional Reflectance Distribution Function

The BRDF defines how may light from an illumination direction $\overrightarrow{\omega_i}(\theta_i, \phi_i)$ is reflected by a surface and into an observation direction $\overrightarrow{\omega_e}(\theta_e, \phi_e)$. θ_i, ϕ_i (respectively, θ_e, ϕ_e) are the zenith and azimuth angle of the light source (respectively, the observer). The BRDF definition was definitively introduced by [9] as :

$$f_r(\overrightarrow{\omega_i}, \overrightarrow{\omega_e}) = \frac{dL_e(\overrightarrow{\omega_e})}{dE_i(\overrightarrow{\omega_i})} = \frac{dL_e(\overrightarrow{\omega_e})}{L_i(\overrightarrow{\omega_i})\cos\theta_i d\overrightarrow{\omega_i}} \quad (3)$$

where L = luminance
E = illuminance

Generally, the reflection is considered as a cumulated effect of several phenomena. The BRDF is usually composed in two terms : a specular term which is modified by the surface roughness and a diffusive term (Lambertian) modeling the multiple reflections between the material micro-facets. The combination of these components provides the global material response to the incident light.

However, except for mirrors, the specular term is not used. It is replaced by a model of the reflection in a preferential direction, called lobe directional-diffus (Figure 1).

Many models have been proposed to describe the BRDF, (cf. [10] for an overview). In this study, the Lafortune model is selected. Even it is quite simple and computationally efficient, it allows us to reproduce the complex reflectance of wet and dry road surfaces [11], [12].

Based on the Phong model [13], Lafortune proposed an empirical model [14], decomposed in a sum of lobes. Each lobe is given by :

$$f_r(\theta_i, \phi_i, \theta_e, \phi_e) = \rho\frac{n+2}{2\pi}\max(\cos\xi', 0)^n \quad (4)$$

where ξ' = angle between the observation and specular direction

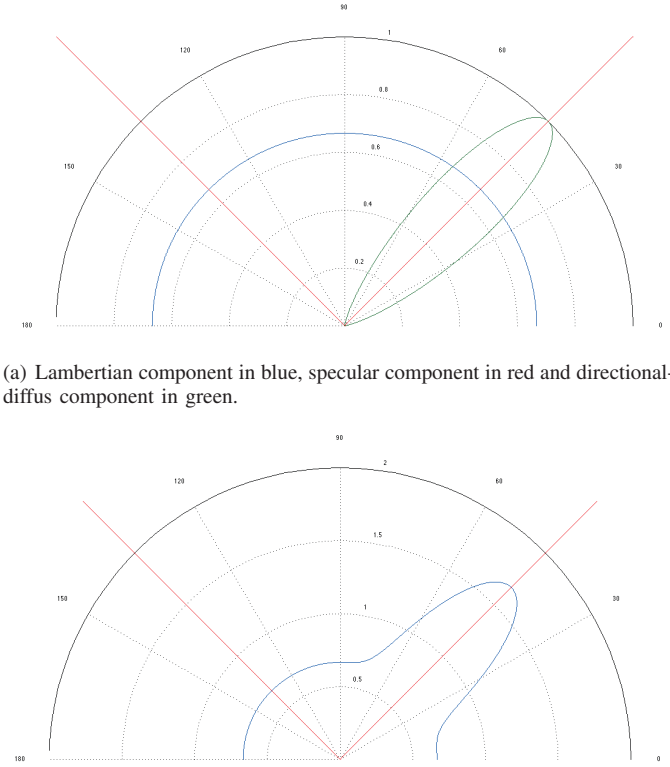

(a) Lambertian component in blue, specular component in red and directional-diffus component in green.

(b) Sum of BRDF components

Fig. 1. Plot of BRDF components of Lafortune model

ρ = albedo
n = specular reflectivity

When $n = 0$, we find the Lambert model and when $n \to \infty$ we have the mirror's model. We can rewrite it using a Householder matrix :

$$f_r(\theta_i, \phi_i, \theta_e, \phi_e) = \rho\frac{n+2}{2\pi}\max(\overrightarrow{R}.\overrightarrow{\omega_e}, 0)^n \quad (5)$$

$$= \rho\frac{n+2}{2\pi}\max(\overrightarrow{\omega_i}^T(2\overrightarrow{N}\overrightarrow{N}^T - I)\overrightarrow{\omega_e})^n \quad (6)$$

where $\overrightarrow{R}$ = specular direction
$\overrightarrow{N}$ = normal to the surface
I = identity matrix

In order to generalize Equation 6, the Householder transform can be replaced by a general 3×3 matrix M :

$$f_r(\theta_i, \phi_i, \theta_e, \phi_e) = \rho\max(\overrightarrow{\omega_i}^T M\overrightarrow{\omega_e}, 0)^n \quad (7)$$

with $M = \frac{n+2}{2\pi}(2\overrightarrow{N}\overrightarrow{N}^T - I)$.

The reciprocity criteria implies : $M = M^T$.

A singular value decomposition of M into $Q^T DQ$ is applied. Q corresponds to the geometrical transformation into a new local coordinate system, where the matrix M is simplified into a diagonal matrix D. Then, the axes are

aligned with the normal and to the principal directions of anisotropy. Thus, the BRDF becomes:

$$f_r(\vec{\omega_i},\vec{\omega_e}) = \rho \max(C_x\omega_{e_x}\omega_{i_x} + C_y\omega_{e_y}\omega_{i_y} + C_z\omega_{e_z}\omega_{i_z}, 0)^n \quad (8)$$

where C_x, C_y, C_z = diagonal coefficient of the matrix D

The Equation 8 defines one lobe shape. For representing complex real-life reflectance functions, Lafortune calculates a sum of several primitive functions of the form of Equation 8:

$$f_r(\vec{\omega_i},\vec{\omega_e}) = \max\left(\sum_i \rho_i \left[C_{x,i}\omega_{e_x}\omega_{i_x} + C_{y,i}\omega_{e_y}\omega_{i_y} + C_{z,i}\omega_{e_z}\omega_{i_z}\right]^{n_i}, 0\right) \quad (9)$$

D. Rendering equation

Using the models presented in Sections II-B and II-C, we can compute a luminance value for an observation direction thanks to the rendering equation defined by :

$$L(x,\omega_e) = \int_\Omega f_r(x,\omega_i,\omega_e) L_i(x,\omega_i)(\omega_i \cdot n) d\omega_i \quad (10)$$

where Ω = illumination direction of sky
f_r = Lafortune's model
L_i = sky luminance
n = normal to the surface

Thus, using hypothesis on road reflectance properties, we are able to simulate an embedded luminance image of a driving scene. Such an image depends of the date, the hour, the weather and the vehicle direction.

III. Results

We have simulated images of dry and wet roads relying on the rendering equation 10 using different parameters: sky luminance properties, date, hour and vehicle direction.

a) Road BRDF: The wet road have a thin layer of water on the surface. This layer have similar BRDF properties to an imperfect mirror. Thus, the specular property of a wet road is more important than a dry road. In order to model such roads, we choose the BRDF Lafortune parameters presented in table I. The choice of these parameters is based on the IFSTTAR know how.

TABLE I
Parameters setting for Lafortune's BRDF for dry and wet road

Lafortune's parameters	Dry road	Wet road
ρ_d	0.2	0.2
ρ_s	0.3	0.8
C_x	-1	-1
C_y	-1	-1
C_z	1	1
n	5	15

with ρ_d = diffuse reflectance
ρ_s = specular reflectance

Notice that $C_x = C_y$, corresponding to isotropic directional-diffus lobe. Moreover, these parameters are negative to avoid backscattering lobes. Finally, the main differences between wet and dry roads BRDF appears in ρ_s and n parameters, corresponding to the forward scattering lobe form.

b) Sky luminance properties: Using measured data from meteorological station during one year [15], we have plotted Δ versus ε, defined in section II-B in Figure 2.

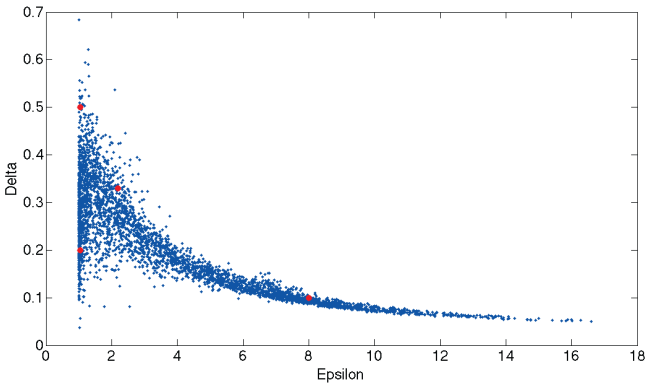

Fig. 2. Δ versus ε

This plot helped us to select four pairs of (ε,Δ), each pair defines one type of sky. We represented in the Table II the different chosen couples and marked it by red dot in Figure 2.

TABLE II
Pairs of (ε,Δ) selected

Type of sky	(ε,Δ)
strongly covered, dark sky	(1.05 , 0.2)
strongly covered, bright sky	(1.05 , 0.5)
almost uncovered, bright dark sky	(2.2 , 0.33)
totally uncovered, dark sky	(8 , 0.1)

c) Date and hour: We compute the sun position thanks to II-A at four dates and for five different times represented in Table III. The positions are defined by the 2 angles (θ,ϕ) in degrees for an observer located in Versailles area (France, (48.7820N, 2.1019E)).

TABLE III
Position of the sun as a function of date and hour

	20/03	21/06	22/09	21/12
7h	(89, 90)	(81, 64)	(97, 81)	(105, 107)
10h	(62, 127)	(52, 97)	(68, 116)	(81, 144)
12h	(50, 160)	(33, 128)	(53, 146)	(73, 168)
14h	(50, 199)	(25, 183)	(48, 185)	(73, 196)
17h	(70, 246)	(44, 252)	(64, 236)	(91, 234)

d) Vehicle direction: Four orientation values $(0°, 90°, 180°, 270°)$ are considered corresponding to the four cardinal direction.

Finally, for each of all those data, we compute an image of a dry road and an image of a wet road. An exemple of such a couple is presented in Figure 3. The sky color is determinate thanks to the Perez model. The dark regions are due to the wide range of sky luminance. The rendering equation is only computed on the road region. To produce these images, we used the Lafortune parameters, defined in Table I. The vehicle is oriented toward the East on the 21th of June at 7:00 am. A totally uncovered and dark sky is used. The position of the sun is represented for indicative purpose by a yellow disk. The difference between the two images appears in the forward scattering property of the wet road surface.

Thus we have built a database containing 640 images.

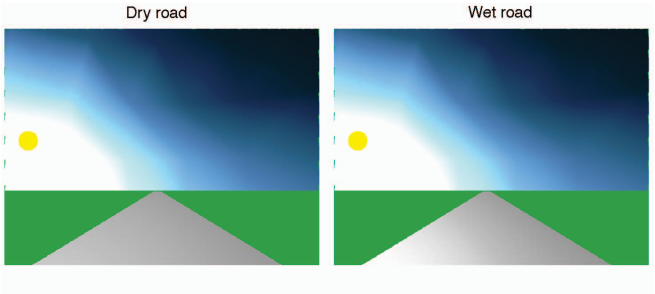

Fig. 3. The first image illustrates a dry road ; the second one, a wet road. The parameters use are : cap = East, date = 21th June, hour = 7 am, ε = 8, Δ = 0.1.

e) Is a wet road discernable from a dry road ?: An euclidienne distance of all road pixels is computed between each couple of images (dry and wet road). We compute an analysis of variance (ANOVA) to determine which parameter and which couple of parameters ((ε, Δ), Date, Hours, Orientations) are the most significant. The protocole is resumed in Figure 4 and the results are exposed in the Table IV.

TABLE IV
ANOVA'S RESULTS

Source	Sum Sq.	d.f.	M. Sq.	F	Prob > F
Date	29.02	3	9.6	1.06	0.3679
Hour	83.67	4	20.9	2.29	0.0607
Weather	179.02	3	59.6	6.52	0.0003
Cap	694.52	3	231.5	25.31	0
Date*Hour	96.87	12	8.0	0.88	0.5655
Date*Weather	115.03	9	12.7	1.4	0.1899
Date*Cap	111.88	9	12.4	1.36	0.2075
Hour*Weather	164.92	12	13.7	1.5	0.1236
Hour*Cap	1681.94	12	140.1	15.32	0
Weather*Cap	316.34	9	35.1	3.84	0.0001
Error	2222.81	243	9.1		
Total	5696.01	319			

According to the Table IV, only the 2 parameters Weather and Cap induce significant differences between images

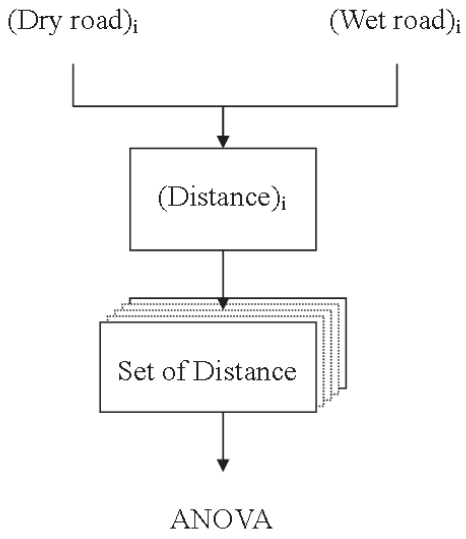

Fig. 4. Protocol to compute ANOVA

($P < 0.05$). The parameter Hour induce a slight variation between wet and dry road images. Finally, the date does not influence our ability to distinguish between dry an wet road. These results are illustrated in the box plot of Figure 5 to 8.

In Figure 5, we may notice that under a strongly covered and dark sky, the difference between wet and dry is high and have a very small variability, thus it is always easy to distinguish the 2 roads. This could be explain by the fact that the sun is not visible and the specular effect is absent. Then, only the intensity of the road is taken into account. On the contrary with an uncovered sky, the detection could be harder or easier, depending of the other parameters.

In Figure 6, we constate that the distance between dry and wet with parameter North is smaller than the parameter East, South or West. It is due to the fact that the observed surface is never between the vehicle and the main light source. Thus, when the vehicle is oriented toward the North, it will seem that it will be more difficult to differentiate the 2 roads.

In Figure 7, it appears that the distance fluctuate slightly according to the parameter Hour. Thus, depending on the others parameters, it will be more or less easily to detect the wet roads. On the contrary, as is shown in Figure 8, the parameter Date will not be determinant in the distinction of wet or dry surfaces.

Looking for parameters couple, it appears that only (Hour,Cap) and (Weather,Cap) are significant.

Figures 9 and 10 illustrate the impact of vehicle's heading according to the hour and the weather parameter.

In Figure 9, we could verify that if a vehicle is oriented toward the East, the difference between dry and wet road images is most important in the morning than in the evening. On the contrary, when the vehicle is oriented toward the West, the difference is higher in the evening than in the morning. Moreover, when the vehicle is oriented toward the

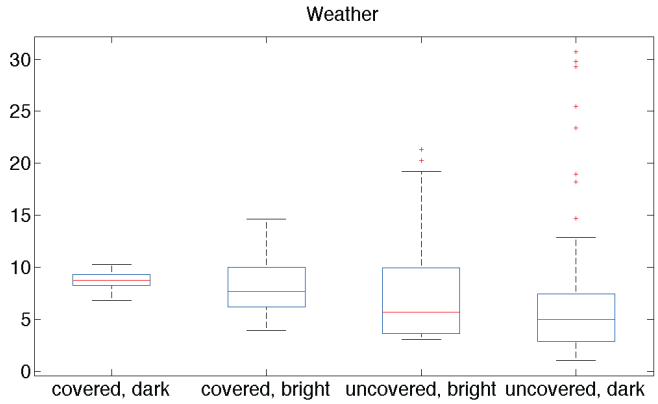

Fig. 5. Distance variability of parameter Weather

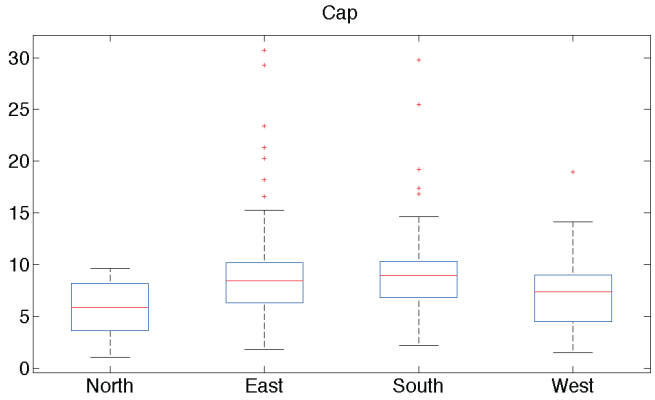

Fig. 6. Distance variability of parameter Cap

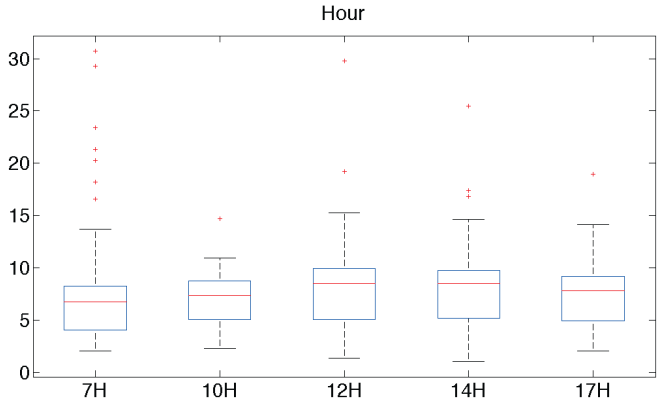

Fig. 7. Distance variability of parameter Hour

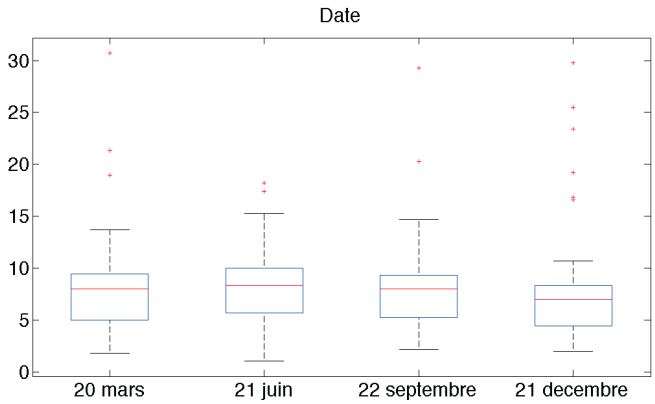

Fig. 8. Distance variability of parameter Date

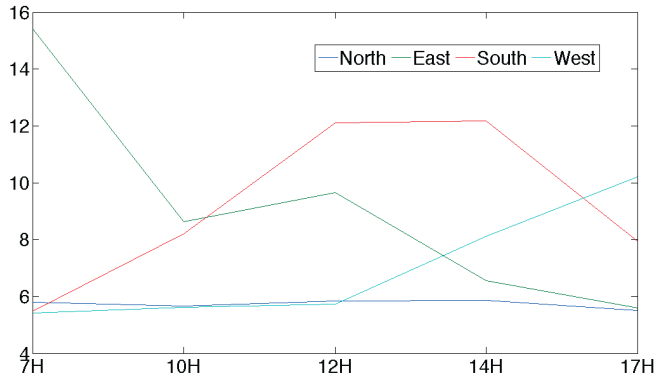

Fig. 9. Impact of the vehicle's heading according to the parameter Hour

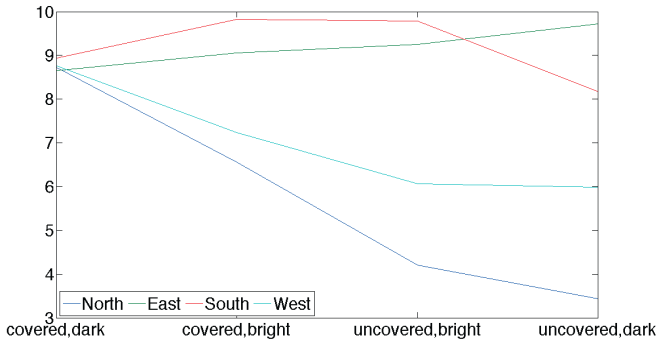

Fig. 10. Impact of the vehicle's heading according to the parameter Weather

North, it seems difficult to differentiate the 2 types of road. These results can be explained by the fact that the difference between dry and wet surface would be easiest to distinguish if the main light source is in our field of view. In this case, it induces forward scattering effect that are quite different for dry and wet surfaces. This is illustrated in Figure 3. The wet road behavior is similar to an imperfect mirror. This explains why a specular area on the road appears in the trajectory between the sun and the camera. This specular area brings informations about the observed object.

Figure 10 revealed that under a strongly covered and dark sky, we will be able to differentiate the 2 roads regardless the vehicle orientation. We can assumed that the vehicle's heading is not significant under adverse meteorological conditions because this type of sky has not a privileged illuminance direction and it is very dark. Moreover, when the vehicle is oriented toward the South or East, it seems that we will able to detect wet road surface despite the meteorological conditions. On the contrary, under uncovered sky, when the vehicle is oriented toward the North or West the distinction

between the 2 roads seems harder.

Our objective is to evaluate if we will be able to retrieve the physical state of the road. Then, we consider that the current image and all other properties (sky luminance, date and cap) are well known, and we try to determine the road BRDF parameters. For this purpose, we apply standard nonlinear Levenberg-Marquardt Algorithm optimization [16], to fit the Lafortune model and retrieve its parameters $(\rho_d, \rho_s, C_x, C_y, C_z, n)$. We present here this approach on one image extracted from our database: the vehicle is oriented toward the East the 21th June at 7:00 am, $\varepsilon = 8$ and $\Delta = 0.1$. The initialization parameters are presented in Table V. Because road scatters light into forward direction, we initialize the C_x and C_y parameters to negative values. For the ρ_d and ρ_s parameters, we use the average of ρ value ($\rho \in [0,1]$). The results of Levenberg-Marquardt Algorithm, presented in Table V, shows that all Lafortune parameters are quite well estimate. It will be possible, in this case to distinguish dry and wet road.

TABLE V
RESULTS OF LEVENBERG-MARQUARDT ALGORITHM

Parameters	True	Initial	Fit
ρ_d	0.2	0.5	0.2559
ρ_s	0.8	0.5	0.8609
C_x	-1	-0.5	-0.9903
C_y	-1	-0.5	-1
C_z	1	0.5	1
n	15	10	19.9064

The first results of this study are promising. This method may be able to detect a wet road under some conditions such as the vehicle's heading, the hour, the meteorological conditions.

IV. DISCUSSION AND CONCLUSION

In this paper, we have presented a study with the main objective of determining the significant parameters to do the distinction between wet and dry road by using synthesizes images in an empty environment (an environment without surrounding objects likes building). In other words, we would like to know our capability to predict the real state of the road.

We have shown that the most important parameters are vehicle's heading, weather and hour. The date doesn't have a discriminant character. Thus it is possible to detect wet roads regardless the date. Thanks to this study, we know the favorable cases to detect the wet roads. In other words, we could wait a favorable vehicle orientation to seek for the road state.

We propose a wet/dry road detection approach based on estimating the bidirectional reflectance distribution function of road surfaces by Levenberg-Marquardt Algorithm optimization. We utilize the Lafortune model that considers diffuse and specular reflection characteristics. Concerning the road conditions in night time, the headlights reflection on the road can be observed. Knowing that the headlights position is well known, we can find the backscatter characteristics of the road. On the one hand, these results would be useful to improve road marking detectors. Indeed, such detectors are often disturbed by specular areas in particular for wet roads. On the other hand, by detecting the road state, we may produce an alert to the driver if his behavior is inappropriate to the current driving conditions.

Future work will include a study on the accuracy of Levenberg-Marquardt Algorithm optimization. Moreover, we will work on a classification method on BRDF estimated properties. We will hope to extend our approach to frozen roads, indeed they are more specular than wet road. Finally, we pan to apply our method both to synthetic and real scene images.

REFERENCES

[1] I. Reda and A. Andreas, *Solar position algorithm for solar radiation applications*, U. D. of Energy Laboratory, Ed. National Renewable Energy Laboratory, 2003.

[2] R. Grena, "An algorithm for the computation of the solar position," *Solar Energy*, vol. 82, no. 5, pp. 462–470, 2008.

[3] T. Van Flandern and K. Pulkkinen, "Low-precision formulae for planetary positions," *The Astrophysical Journal Supplement Series*, vol. 41, pp. 391–411, 1979.

[4] CIE, "Spatial distribution of daylight-cie standard general sky," *CIE S*, vol. 11, 2003.

[5] J. Wright, R. Perez, and J. Michalsky, "Luminous efficacy of direct irradiance: Variations with insolation and moisture conditions," *Solar Energy*, vol. 42, no. 5, pp. 387 – 394, 1989.

[6] R. Perez, P. Ineichen, R. Seals, J. Michalsky, and R. Stewart, "Modeling daylight availability and irradiance components from direct and global irradiance," *Solar energy*, vol. 44, no. 5, pp. 271–289, 1990.

[7] R. Perez, R. Seals, and J. Michalsky, "All-weather model for sky luminance distribution-preliminary configuration and validation," *Solar Energy*, vol. 50, no. 3, pp. 235 – 245, 1993.

[8] ——, "Erratum to "all-weather model for sky luminance distribution-preliminary configuration and validation"," *Solar Energy*, vol. 51, no. 5, p. 423, 1993.

[9] F. Nicodemus, J. Richmond, and H. J.J, *Geometrical considerations and nomenclature for reflectance*, d, Ed. US Department of Commerce, National Bureau of Standards Washington, D. C, 1977, vol. 160.

[10] R. Montes Soldado and C. Ureña Almagro, "An overview of brdf models," 2012.

[11] Y. Yu and J. Malik, "Recovering photometric properties of architectural scenes from photographs," in *Proceedings of the 25th annual conference on Computer graphics and interactive techniques*. ACM, 1998, pp. 207–217.

[12] W. Matusik, "A data-driven reflectance model," Ph.D. dissertation, Citeseer, 2003.

[13] B. Phong, "Illumination for computer generated pictures," *Communications of the ACM*, vol. 18, no. 6, pp. 311–317, 1975.

[14] E. Lafortune, S. Foo, K. Torrance, and D. Greenberg, "Non-linear approximation of reflectance functions," in *Proceedings of the 24th annual conference on Computer graphics and interactive techniques*. ACM Press/Addison-Wesley Publishing Co., 1997, pp. 117–126.

[15] NCDC, "National climatique data center," http://www.ncdc.noaa.gov, 2004.

[16] D. W. Marquardt, "An algorithm for least-squares estimation of nonlinear parameters," *Journal of the Society for Industrial & Applied Mathematics*, vol. 11, no. 2, pp. 431–441, 1963.